The Role of Network Architecture on the Glass Transition Temperature of Epoxy Resins

ALAN J. LESSER, EMMETT CRAWFORD

Polymer Science and Engineering Department, University of Massachusetts, Amherst, Massachusetts 01003

Received 8 October 1996; accepted 17 April 1997

ABSTRACT: A series of epoxy networks were synthesized in which the molecular weight between crosslinks (M_c) and crosslink functionality were controlled independent of the network chain backbone composition. The glass transition temperature (T_g) of these networks was found to increase as M_c decreased. However, the rate at which T_g increased depended on crosslink functionality. The dependency of M_c on T_g is well described by two models, one based on the concept of network free volume while the other model is based on the principle of corresponding states. Initially, neither model could quantitatively predict the effect of crosslink functionality in our networks. However, our tests indicated that both the glass transition and the rubbery moduli of our networks were dependent on M_c and crosslink functionality, while the glassy state moduli were independent of these structural variables. The effect of crosslink functionality on the rubbery modulus of a network has been addressed by the front factor in rubber elasticity theory. Incorporation of this factor into the glass transition temperature models allowed for a quantitative prediction of T_g as a function of M_c and crosslink functionality. © 1997 John Wiley & Sons, Inc. J Appl Polym Sci **66:** 387–395, 1997

Key words: network architecture; glass transition temperature; epoxy resins

INTRODUCTION

The glass transition temperature (T_g) is one of the most important properties of a polymeric system. It has been shown in epoxy resins that the yield and fracture behavior are related to the glass transition temperature.[1–3] Hence, it is important to understand the role that network architecture plays on T_g such that performance properties can be tailored. Models propose that the T_g of a fully reacted polymer network (T_{gx}) is a result of two factors: T_g of the linear polymer backbone at infinite molecular weight ($T_{g\infty}$) and the increase in T_{gx} due to crosslinking.[4–7] However, none of these models directly account for junction point functionality, which has been shown to affect T_g.[8]

In the present work, epoxy networks were constructed in which the molecular weight between crosslinks and crosslink functionality were controlled without significantly affecting $T_{g\infty}$. The effect of M_c and crosslink functionality on the glassy moduli, rubbery moduli, and T_g of these networks were determined experimentally. Observations and correlations of these properties allowed for an empirical modification of two popular glass transition temperature models to quantitatively account for crosslink functionality.

EXPERIMENTAL

Materials

Epon 825, a diglycidyl ether of bisphenol A epoxy resin, was supplied by Shell Chemical Company.

Correspondence to: A. Lesser.
Contract grant sponsor: National Science Foundation.
Contract grant sponsor: G. E. Plastics.
Contract grant sponsor: Monsanto.
Contract grant sponsor: Shell Foundation.

Journal of Applied Polymer Science, Vol. 66, 387–395 (1997)
 CCC 0021-8995/97/020387-09

Table I Chemical Structures of Resin and Curing Agents

Epon 825: A diglycidyl ether of bisphenol A epoxy resin

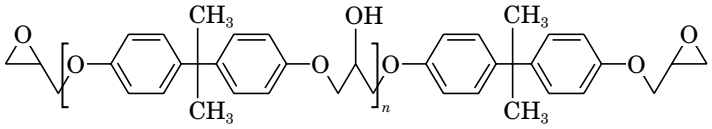

Crosslinking Agents

Ethylenediamine (EDA)

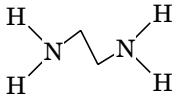

N-Methylethylenediamine (MEDA)

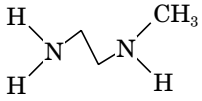

Chain Extender

N,N′-Dimethylethylenediamine (DMEDA)

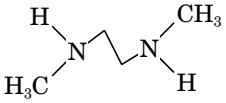

Epon 825 has an epoxy equivalent weight of 175 g/mol of epoxide groups. This value corresponds to $n = 0.04$ in the structure of Epon 825 shown in Table I.

Ethylenediamine (EDA), *N*-methylethylenediamine (MEDA), and *N,N′*-dimethylethylenediamine (DMEDA) were purchased from Aldrich Chemical Company with a minimum purity of 99.0%. The structures of these amine molecules can be found in Table I. EDA is modeled as a tetrafunctional crosslink and MEDA is modeled as a trifunctional crosslink, while DMEDA is modeled as a chain extender. By blending different amounts of these amines, M_c and crosslink functionality can be controlled while maintaining stoichiometry.

1,4-Diaminobutane, hexamethylenediamine, 1,8-diaminooctane, 1,10-diaminodecane, and 1,12-diaminododecane were also purchased from Aldrich Chemical Company with a minimum purity of 99.0%. Stoichiometric amounts of these crosslinking agents were mixed with Epon 825. These amine molecules were selected to determine whether short chain diamines, like ethylenediamine, can achieve high conversions despite a reduction of segmental mobility due to a high degree of crosslinking. All materials were used as received without further purification.

Sample Preparation

Epon 825 was degassed in a vacuum oven at 100°C for 8 h. After degassing, the resin was placed in a oven at 50°C and allowed to equilibrate. Stoichiometric amounts of the amines were mixed with the resin for 3 min and degassed for an additional 5 min. The mixture was then poured into treated 11.5-mm diameter glass test tubes, and between two treated glass plates, which were separated by a 1.6-mm thick Teflon spacer and clamped with several c-clamps. The glass was pretreated with SurfaSil, a silating agent purchased from Pierce Chemical Company, which prevents adhesion between the resulting resin plaque and the glass. Once the resin was poured, the mold and test tubes were placed back into the oven at 50°C for 3 h for gelation to occur. The molds and test tubes were then placed in an oven and postcured for 3 h at a temperature 20°C above T_{gx}, as determined by a differential scanning calorimeter (DSC). After postcure, the plaques and test tubes were allowed to slowly cool to room temperature and then separated from the glass. Samples (5–10 mg) taken from the plaques were analyzed by a DSC while rectangular bars, machined from the plaques using a specially designed router, were analyzed by a dynamic mechanical thermal analyzer (DMTA). The test tubes were broken and the resulting epoxy cylinders were cut with a diamond saw to form 20-mm long compression samples. All samples were placed in a desiccator 1 week prior to testing.

Mechanical and Thermal Analysis

Differential scanning calorimetry was performed with a DuPont Thermal Analyzer 2000. The T_gs of all synthesized networks were measured at a

heating rate of 10°C/min. Dynamic mechanical thermal analysis was performed with a Polymer Laboratories' DMTA in the single cantilever mode operating at 1 Hz and at a heating rate of 2°C/min. Compression tests of all networks were performed at 20 K above T_{gx} and at a crosshead speed of 0.5 mm/min with a Model 1123 Instron. The compression samples were compressed to 75% of their original height. In all static compression tests, little to no mechanical hysterisis occurred between compressing and decompressing the samples. This indicated that equilibrium was achieved and that application of rubber elasticity theory to evaluate the networks is valid.

RESULTS AND DISCUSSION

Calculation of Network Parameters

In what follows, we assume that all network formation occurs by the reaction of epoxide groups with primary and secondary amines and that full conversion is achieved. This allows important network parameters to be calculated. This consideration is supported by the fact that reactions of epoxide groups with primary and secondary amines are more favored than the base catalyzed epoxide etherfication reaction, which does not occur until reaction temperatures are much greater than 150°C.[9,10] In addition, full conversion is supported by the observation that the glass transition temperature of the constructed networks did not change with a further increase in postcure time and postcure temperature.[5]

Horie et al.[11] argued that an increase in the number of methylene units in aliphatic diamines of the structure $H_2N—(CH_2)_n—NH_2$ reacted with a diglycidyl ether of bisphenol A epoxy resin results in an increase in the final conversion, with near 100% conversion being achieved by diamines with six or more methylene units. In their study, the supposed lack of high conversions in shorter amines was attributed to the restriction of segmental mobility due to high levels of crosslinking. However, our work does not support this finding. In Figure 1, we present a plot of T_{gx} vs. the number of methylene units for networks constructed with Epon 825 and a homologous series of aliphatic diamines of the structure $H_2N—(CH_2)_n—NH_2$. Assuming 100% conversion occurred for networks constructed by diamines with six or more methylene units, Horie et al.[11] findings would suggest a plateau in T_{gx} as the number of methylene units approaches three to four. Our results show that

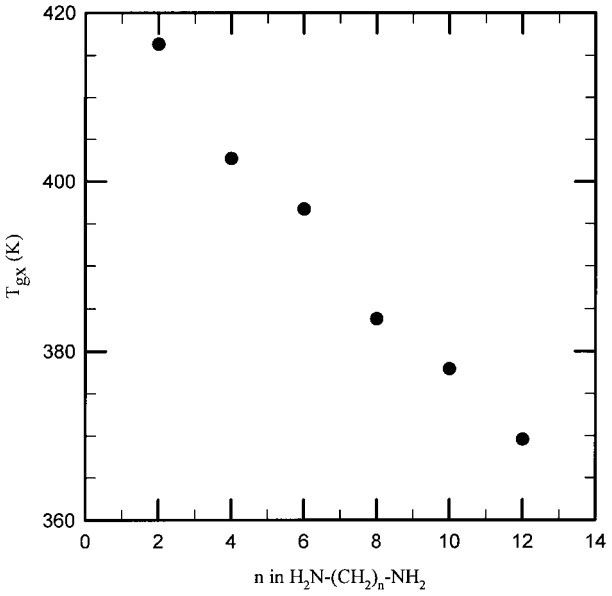

Figure 1 The variation in T_{gx} as a function of the number of methylene units for networks constructed with Epon 825 and a homologous series of aliphatic diamines as determined by DSC.

no plateau exists, indicating that high degrees of conversion might be possible in resins cured with short chain diamines. Another interesting observation in our laboratory is the fact that samples cured with EDA in a DSC pan resulted in a much lower T_g than the same samples cured between glass plates. This discrepancy could be the result of EDA consumption in the DSC pan by side reactions with the pan and air. Because the glass transition temperature is connected with network conversion, this observation could help explain the lack of high conversions by networks cured with EDA as reported by Horie et al.[11] Vakil and Martin[12] reported a conversion of 95% for a network synthesized with Epon 825 and 1,3-phenylenediamine subjected to a similar postcure schedule as our networks. The extent of reaction in their study was determined by infared spectroscopy. However, it is usually difficult to accurately determine the extent of reaction for the final few percentage of reactive groups.[13] Taking this into account, Wisanrakkit and Gillham[14] proposed using the glass transition temperature to monitor the extent of reaction because it is extremely sensitive to the network structure changes occurring in the final stages of the curing process. Wisanrakkit and Gillham[14] showed that when the glass transition temperature did not change with an increase in postcure time or postcure temperature that the reaction had reached full conversion. In their study,

a diglycidyl ether of bisphenol A epoxy resin was reacted with a commercial aromatic curing agent. Because aliphatic amines are in general more reactive than aromatic amines[13] and it was found experimentally that the glass transition temperature of our networks did not change with an increase in postcure time and postcure temperature, the assumption of full conversion seems reasonable.

Making use of our findings, the average molecular weight per crosslink (M_{pc}) was calculated for the networks constructed with EDA, MEDA, and DMEDA by using the following equation:

$$M_{pc} = \frac{M_e + \sum_{f=2}^{\infty} \frac{M_f}{f} \Phi_f}{\sum_{f=3}^{\infty} \frac{\Phi_f}{f}} \quad (1)$$

where M_e is the epoxide equivalent weight of the resin, f is the functionality of the amine, M_f is the molecular weight of the fth functional amine, and ϕ_f is the mol fraction of amine hydrogens provided by the fth functional amine. By definition the crosslink density is inversely proportional to M_{pc}. The crosslink density can alternatively be defined in terms of the mol fraction of the monomer units, which act as crosslinks. Equation (2) was used to evaluate the molar crosslink density (X_m).

$$X_m = \frac{\sum_{f=3}^{\infty} \frac{\Phi_f}{f}}{\left(\frac{1}{2} + \sum_{f=2}^{\infty} \frac{\Phi_f}{f}\right)}. \quad (2)$$

The average molecular weight between crosslinks (M_c) was calculated by determining the average crosslink functionality (f_{cav}) and the average molecular weight per crosslink (M_{pc}).

$$f_{\text{cav}} = \frac{\sum_{f=3}^{\infty} \Phi_f}{\sum_{f=3}^{\infty} \left(\frac{\Phi_f}{f}\right)} \quad (3)$$

$$M_c = \frac{2}{f_{\text{cav}}} M_{pc}. \quad (4)$$

These network parameters were calculated such that the theories describing the increase in T_{gx} due to crosslinking could be evaluated for networks constructed with EDA, MEDA, and DMEDA.

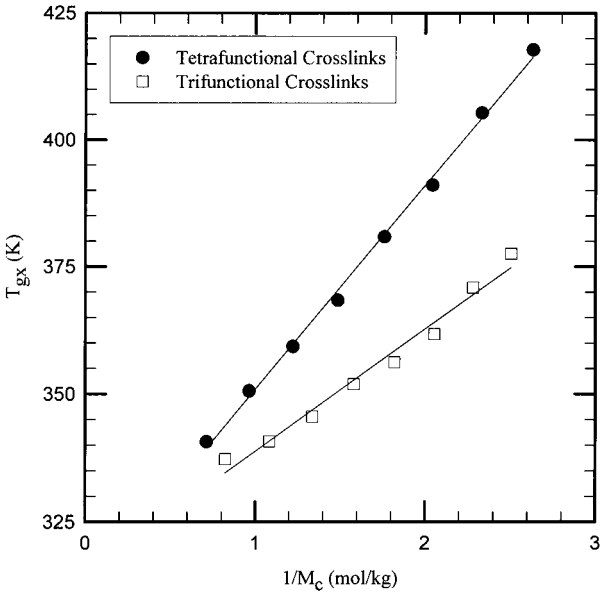

Figure 2 The variation in T_{gx} as a function of $1/M_c$ for networks constructed with the tetrafunctional crosslinks and trifunctional crosslinks as determined by DSC.

Effects of Crosslinking on the Glass Transition Temperature

In Figure 2, T_{gx} is plotted against $1/M_c$ for networks comprised of tetrafunctional crosslinks, EDA, and networks comprised of trifunctional crosslinks, MEDA. Both networks show an increase in T_{gx} as M_c decreases. However, the rate of increase is greater for tetrafunctional crosslinked networks than trifunctional crosslinked networks. The apparent linear behavior was first described in a semiempirical fashion by Fox and Loshaek.[4] A more recent theory by Banks and Ellis[5] also proposes a linear relationship based on the addition and redistribution of network free volume. In this model, T_{gx} is described by the following equation:

$$T_{gx} = T_{g\infty} + \frac{\zeta}{M_c} \quad (5)$$

where ζ is proportional to the molecular weight of the unreacted resin and to the ratio of incremental free volume contributions from the resin and the curing agent.[12] Linear regression of the data in Figure 2 can be found in Table II. In terms of the network free-volume theory, tetrafunctional crosslinks would have less incremental free volume than trifunctional crosslinks. The value of ζ obtained for the tetrafunctional networks is close to the often-cited value by Neilsen[15] of 39 kg

Table II Linear Regression Results for T_g Data Using Network Free Volume Theory

f_{cav}	ζ (DSC)	$T_{g\infty}$ (DSC)	ζ (DMTA)	$T_{g\infty}$ (DMTA)
3	24 kg K/mol	315 K	21 kg K/mol	324 K
4	40 kg K/mol	311 K	41 kg K/mol	315 K

K/mol. The similar values in $T_{g\infty}$ shown in Table II for our trifunctional networks and tetrafunctional networks support our claim that amine functionality is not affecting the linear polymer backbone. Although the network free-volume theory is effective in analyzing the data, it contains many parameters that cannot be evaluated experimentally.

Another theory used to describe the effect of crosslinking on the glass transition temperature of a polymer network was proposed by DiBenedetto.[6] In this theory, based on the principle of cooresponding states, T_{gx} is described by the following equation:

$$\frac{T_{gx} - T_{g\infty}}{T_{g\infty}} = k \frac{X_m}{1 - X_m} \qquad (6)$$

where k is a universal constant, and X_m is the molar crosslink density.[16] In Figure 3, T_{gx} is plotted against

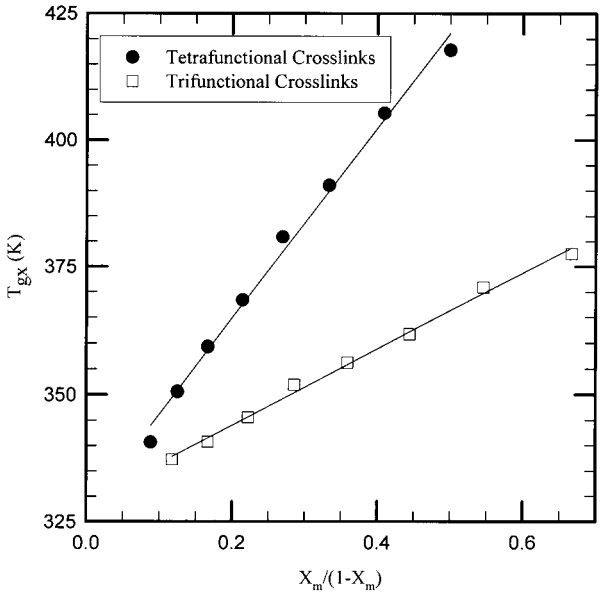

Figure 3 The variation of T_{gx} as a function of $X_m/(1 - X_m)$ for networks constructed with tetrafunctional crosslinks and trifunctional crosslinks as determined by DSC.

$$\frac{X_m}{1 - X_m}$$

for the same network systems used for Figure 2. Linear regression results of the data in Figure 3 can be found in Table III. The k value for the tetrafunctional networks seems reasonable when compared with the data of Stutz et al.,[16] which report k ranging from 0.636 to 0.925 for a variety of network polymers ranging from crosslinked epoxies to natural rubber. However, the value of k for the trifunctional networks falls well below this range.

Neither theory seems to have the ability to quantitatively account for the effect of crosslink functionality on T_{gx}. An attempt to accommodate crosslink functionality was made by Stutz et al.[16] Implicit in their approach, is that T_{gx} is affected by crosslink functionality in the same manner as described by the theory of phantom networks with crosslink mobility.[17] However, Stutz et al. could not test their networks in the rubbery regime to validate their model because their networks were only partially reacted. Another limitation to studying partially reacted networks is the fact that a distribution of crosslink functionality has to be assumed as opposed to our networks in which the crosslink functionality is prescribed.

Dynamic and Static Mechanical Properties

Dynamic mechanical thermal analysis performed on our networks also gives experimental evidence for the relationship of network architecture on T_{gx}. In Figures 4 and 5, log tan δ vs. temperature for the networks are plotted. The primary (α) relaxation, which is identified with long-range segmental motion, is affected by the crosslink density and crosslink functionality of the network. Taking the α peak as T_{gx}, similar plots to those of Figures 2 and 3 can be made. The linear regression results of these data are shown in Table II and Table III for the network free volume theory and the corresponding states theory, respectively. Differences in the DSC T_g data and the DMTA T_g data are the result of differences in the definitions of

Table III Linear Regression Results for T_g Data Using Corresponding States Theory

f_{cav}	k (DSC)	$T_{g\infty}$ (DSC)	k (DMTA)	$T_{g\infty}$ (DMTA)
3	0.23	329 K	0.21	334 K
4	0.57	328 K	0.57	331 K

the glass transition temperature and measurement methods. The secondary (β) relaxation, which is identified with localized motions of chain segments or side chains, does not seem to be significantly affected by changes in M_c or crosslink functionality. The β transition for all networks occurred near 235 K and has been attributed to the glyceryl group in the network structure.[18,19]

In Figures 6 and 7, the log of the storage modulus (E') vs. temperature for the networks are plotted. In both plots, M_c and crosslink functionality display little effect on the glassy modulus. However, these structural variables influence the glass transition temperature of these networks. Quantitative analysis of the rubbery regime of the DMTA data was limited by poor gripping of the samples above T_{gx}, but it can be seen in Figure 6 that crosslink density effects the rubber moduli of these networks.

To obtain better rubber moduli data for all the networks, static compression tests were performed on the networks 20 K above their glass transition temperature. The theory of rubber elasticity provides the following relationship for an ideal network in compression:

$$\frac{\sigma_c}{T(\lambda - 1/\lambda^2)} = g\frac{\rho R}{M_c} \qquad (7)$$

where σ_c is the nominal compressive stress, R is the gas constant, T is temperature, ρ is the polymer density, λ is the compressive ratio, and g is factor that depends on crosslink mobility.[17] In networks where fluctuations of crosslinks occur, $g = (f_{cav} - 2)/f_{cav}$.[20,21] In networks where crosslink fluctuations are suppressed, $g = 1$. Figures 8 and 9 are plots of $-\sigma_c/T$ vs. $-(\lambda - 1/\lambda^2)$ for tetrafunctional crosslinked networks and trifunctional crosslinked networks, respectively. For a given compression ratio, the compressive stress increases with a decrease in M_c. In Figure 10, we present two plots; Figure 10(A) shows the relationship of the average value of $\sigma_c/T(\lambda - 1/\lambda^2)$ determined experimentally for each network vs. g/M_c, with $g = 1$, and Figure 10(B) presents the same data with $g = (f_{cav} - 2)/f_{cav}$. Because the

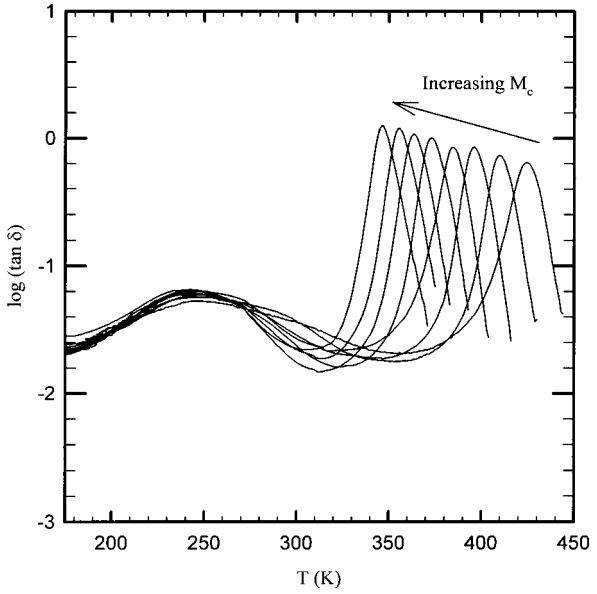

Figure 4 Log(tan δ) as a function of temperature for tetrafunctional crosslinked networks. M_c (g/mol) = 380, 430, 490, 570, 670, 820, 1040, and 1400.

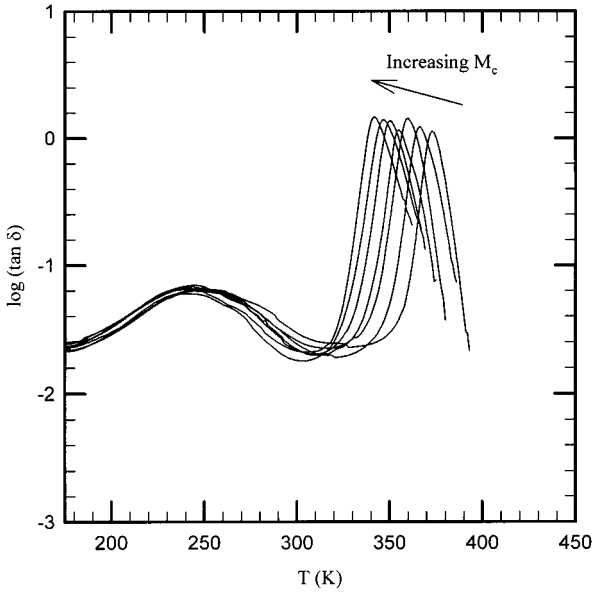

Figure 5 Log(tan δ) as a function of temperature for trifunctional crosslinked networks. M_c (g/mol) = 440, 490, 550, 630, 750, 920, and 1220.

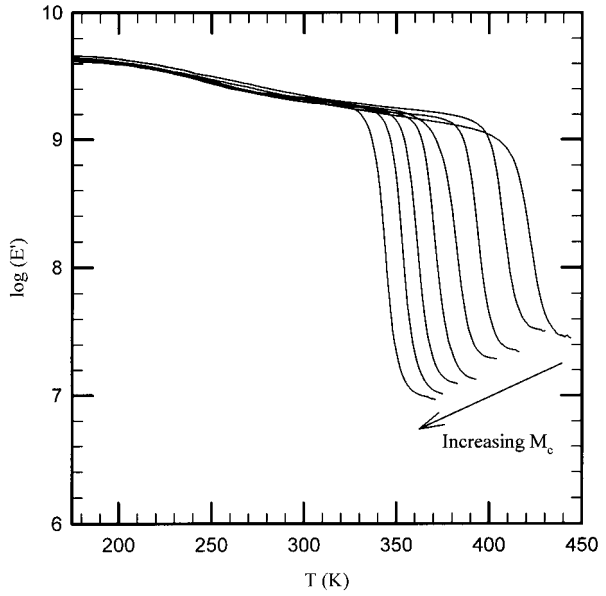

Figure 6 Log (E') as a function of temperature for tetrafunctional crosslinked networks. M_c (g/mol) = 380, 430, 490, 570, 670, 820, 1040, and 1400.

densities of the materials were similar in the rubbery state, the data in Figure 10 indicate that fluctuations of the crosslinks are allowed in these networks.

Incorporation of Crosslink Functionality into the Theories Predicting T_{gx}

The experimental evidence also suggests that the entropic factors that control rubber elasticity also control T_{gx}. Consequently, the two theories describing the effect of M_c on T_{gx} can be modified to account for crosslink functionality. Using a tetrafunctional crosslinked network as a basis, the theory based on network free volume can be expressed as follows:

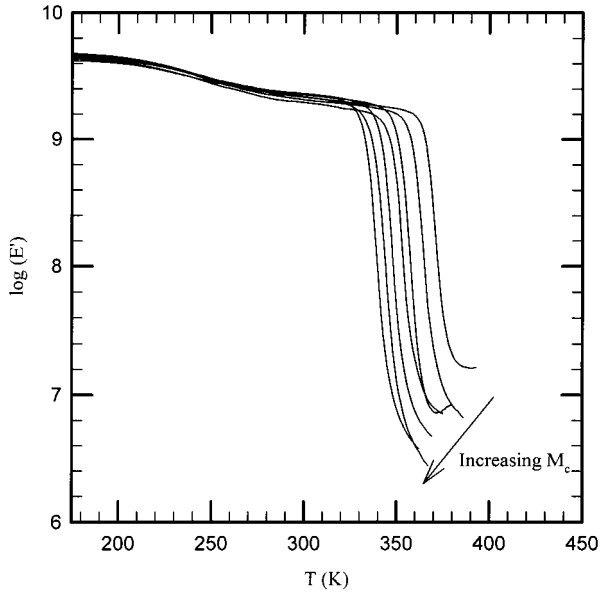

Figure 7 Log (E') as a function of temperature for trifunctional crosslinked networks. M_c (g/mol) = 440, 490, 550, 630, 750, 920, and 1220.

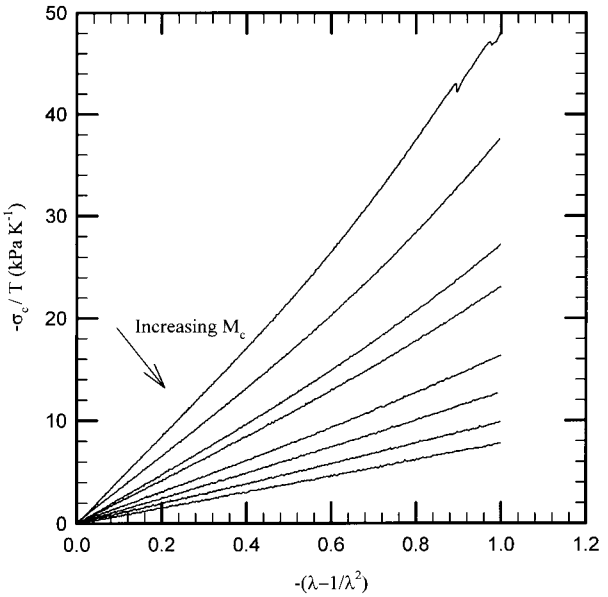

Figure 8 $-\sigma_c/T$ elevated at T_{gx} + 20 K vs. $-(\lambda - 1/\lambda^2)$ for networks comprised of tetrafunctional crosslinks. M_c (g/mol) = 380, 430, 490, 570, 670, 820, 1040, and 1400.

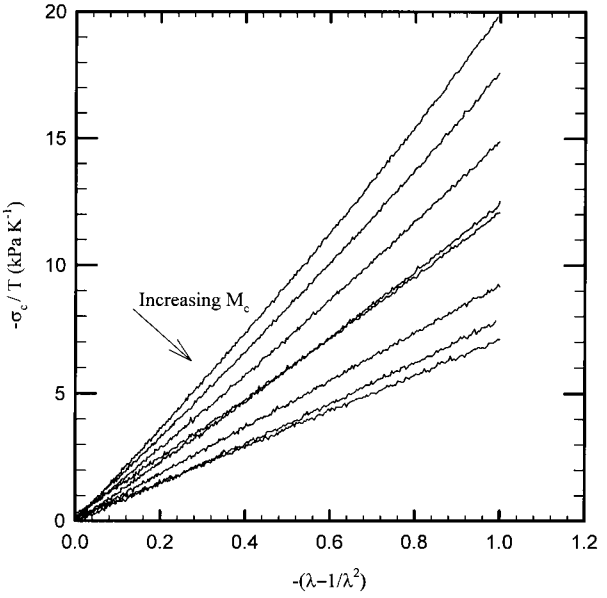

Figure 9 $-\sigma_c/T$ elevated at T_{gx} + 20 K vs. $-(\lambda - 1/\lambda^2)$ for networks comprised of trifunctional crosslinks. M_c (g/mol) = 440, 490, 550, 630, 750, 920, and 1220.

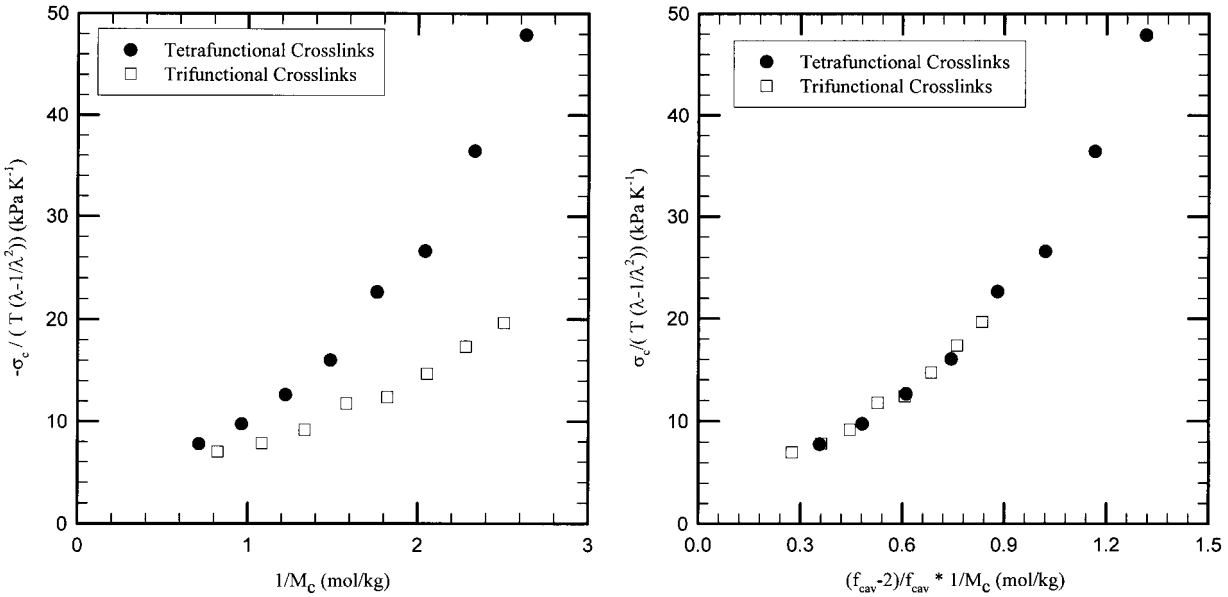

Figure 10 (A) The variation in $\sigma_c/(T(\lambda - 1/\lambda^2))$ as a function of $1/M_c$ for networks comprised of trifunctional crosslinks and tetrafunctional crosslinks. (B) The variation in $\sigma_c/(T(\lambda - 1/\lambda^2))$ as a function of $(f_{cav} - 2)/f^*_{cav}\ 1/M_c$ for networks constructed with tetrafunctional crosslinks and trifunctional crosslinks.

$$T_{gx} = T_{g\infty} + \frac{2(f_{cav} - 2)}{f_{cav}} \frac{\zeta}{M_c} \qquad (8)$$

where the physical interpretation of ζ in eq. (5) has been altered with the free-volume contribution of crosslink functionality now being directly addressed. Figure 11 shows the result of applying eq. (8) to the data. Linear regression of the data in Figure 11 results in ζ = 39 kg K/mol and $T_{g\infty}$ = 311 K. In a similar fashion, the theory based on the principle of corresponding states can be modified by normalizing X_m (X_{mf}). Again, using a tetrafunctional crosslink as the basis, X_{mf} can be expressed as:

$$X_{mf} = \left(\frac{f_{cav}}{2} - 1\right) X_m. \qquad (9)$$

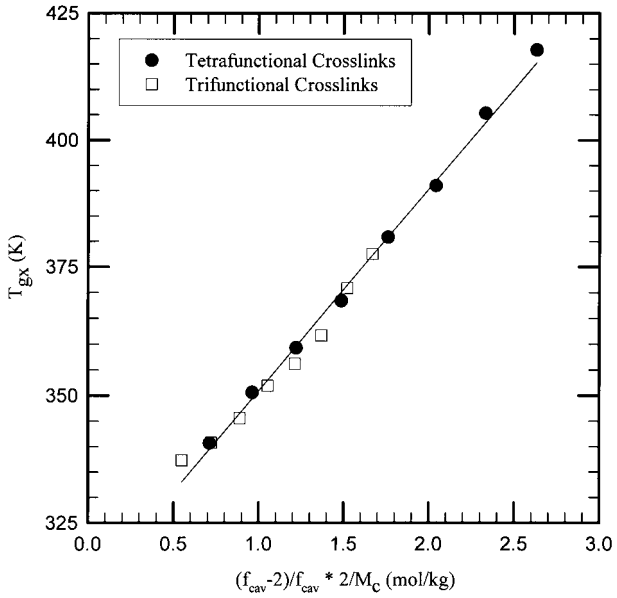

Figure 11 The variation in T_{gx} as a function of $(f_{cav} - 2)/f^*_{cav}\ 2/M_c$ for networks construction with tetrafunctional crosslinks and trifucntional crosslinks as determined by DSC.

Figure 12 shows the results of using X_{mf} to apply eq. (6) to the data. Linear regression of the data in Figure 12 results in k = 0.58 and $T_{g\infty}$ = 328 K. Both Figures 11 and 12 show collapse of the tetrafunctional networks and trifunctional networks onto one single curve with reasonable values of ζ and k for the two models when compared with the literature.

SUMMARY AND CONCLUSIONS

Network polymers were constructed with Epon 825, EDA, MEDA, and DMEDA. The observation that the glass transition temperature of these networks did not change with an increase in postcure time or postcure temperature supported our claim that full conversion was achieved. Making use of this evidence, key network parameters were cal-

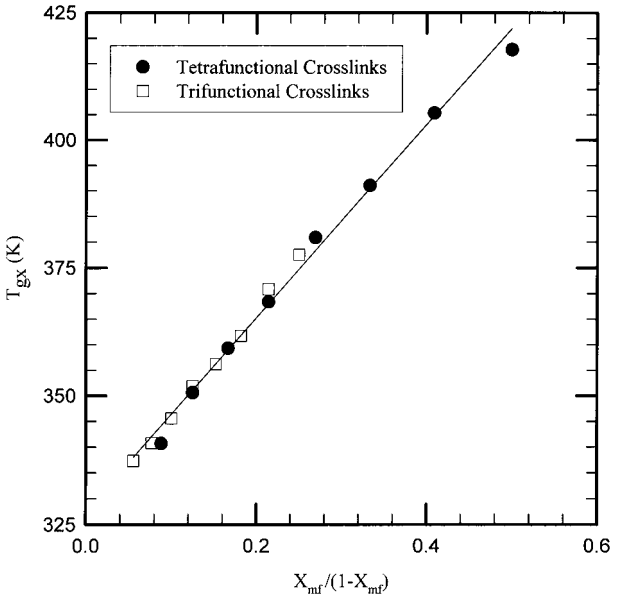

Figure 12 The variation in T_{gx} as a function of $X_{mf}/(1 - X_{mf})$ for networks constructed with tetrafunctional crosslinks and trifunctional crosslinks as determined by DSC.

culated. This approach allowed the molecular weight between crosslinks and crosslink functionality to be controlled independent of the network backbone chain stiffness.

The glass transition temperature of the networks was found to increase when M_c decreased. The rate of increase was greater for networks with tetrafunctional crosslinks than networks with trifunctional crosslinks. Two models, one based on network free volume and the other based on the principle of corresponding states, were able to predict the effect of changing M_c on T_{gx}. However, neither model could quantitatively account for the effect of crosslink functionality.

Dynamic mechanical thermal analysis of the networks showed that the glassy state, including a well known β relaxation, was independent of M_c and crosslink functionality, while the glass transition was dependent on M_c and crosslink functionality. Static compressive tests performed above T_g on our crosslinked resins allowed for a quantitative description of the network structure. The rubbery modulus of our networks could be described by the theory of phantom networks in which the crosslinks are free to fluctuate. This particular model of rubber elasticity takes into account the effect of crosslink functionality. Finally, incorporation of this effect into the two glass transition temperature models allowed for a quantitative prediction of T_g as a function of M_c and crosslink functionality.

The authors gratefully acknowledge the financial support of the National Science Foundation, the Materials Research Science and Engineering Center, along with support from G. E. Plastics, Monsanto, and the Shell Foundation.

REFERENCES

1. W. L. Bradley, W. Schultz, C. Carleto, and S. Komatsu, in *Toughened Plastics I: Science and Engineering,* Vol. 233, C. K. Riew and A. J. Kinloch, Eds., Advances in Chemistry Series, American Chemical Society, Washington, DC, 1993, p. 317.
2. M. Fischer, *Adv. Polym. Sci.,* **100,** 313 (1991).
3. C. Arends, Ed., *Polymer Toughening,* Marcel Dekker Inc., New York, 1996.
4. T. G. Fox and S. Loshaek, *J. Polym. Sci.,* **15,** 371 (1955).
5. L. Banks and B. Ellis, *Polymer,* **23,** 1466 (1982).
6. A. T. DiBenedetto, *J. Polym. Sci. Phys.,* **25,** 1949 (1987).
7. E. A. DiMarzio, *J. Res.,* **68A,** 611 (1964).
8. E. Rietsch, D. Daveloose, and D. Froelich, *Polymer,* **17,** 859 (1976).
9. J. P. Bell, *J. Appl. Polym. Sci.,* **14,** 1901 (1970).
10. E. F. Oleinik, *Adv. Polym. Sci.,* **80,** 49 (1986).
11. K. Horie, H. Hiura, M. Sawads, I. Mita, and H. Kambe, *J. Polym. Sci. A-1,* **8,** 1357 (1970).
12. U. M. Vakil and G. C. Martin, *J. Appl. Polym. Sci.,* **46,** 2089 (1992).
13. B. Ellis, Ed., *Chemistry and Technology of Epoxy Resins,* Chapman & Hall, London, 1993.
14. G. Wisanrakkit and J. K. Gillham, *J. Appl. Polym. Sci.,* **41,** 2885 (1990).
15. L. E. Nielsen, *J. Macromol. Sci., Rev. Macromol. Chem.,* **C3,** 69 (1969).
16. H. Stutz, K. H. Illers, and J. Metes, *J. Polym. Sci. Phys.,* **28,** 1483 (1990).
17. P. J. Flory, *Polymer,* **20,** 1317 (1979).
18. G. A. Pogany, *Polymer,* **11,** 66 (1970).
19. J. G. Williams, *J. Appl. Polym Sci.,* **23,** 3433 (1979).
20. W. W. Graessley, *Macromolecules,* **8,** 186 (1975).
21. J. A. Duiser and A. J. Staverman, in *Physics of Non-Crystalline Solids,* J. A. Prins, Ed., North-Holland Publishing Co., Amsterdam, 1965.